A unified 2D land seismic data analysis workflow

Oz Yilmaz, GeoTomo, Houston, describes a time-with-depth workflow for earth modelling and imaging in areas with irregular topography, complex near-surface, and complex subsurface based on analysis of seismic data in shot-receiver coordinates, not in midpoint-offset coordinates.

Seismic data acquired in areas with irregular topography, complex near-surface, and complex subsurface require a customized analysis workflow. A near-surface is usually defined as a relatively unconsolidated, low-velocity soil column with less than 30 m thickness. Nevertheless, there are many areas where the near-surface thickness and velocities may vary significantly along the seismic line traverses. Additionally, a near-surface zone may include high-velocity outcrops and layers with vertically varying velocities. Such complexity in the near-surface combined with irregular surface topography with significant elevation differences along a line traverse lead us away from conventional processing to an analysis workflow to cope with the following problems associated with the near-surface:

- Analytical methods and linear inversion methods for estimating the near-surface model are limited in their ability to resolve lateral velocity variations because of the assumption that the refractor is locally flat within the spread length. Such *layer-based* methods also assume that the first-arrival times are associated only with refracted waves. As a result, vertical velocity variations with velocity inversion are not resolvable by these methods. To estimate the model for a complex near-surface, you need *grid-based* nonlinear traveltime tomography applied to first-arrivals without restricting the wave type to refracted waves, only. The nonlinear inversion accounts for changes in traveltime gradients which are directly related to velocity variations within the near-surface.
- The vertical-ray assumption in statics corrections is only valid for a thin, low-velocity near-surface. When dealing with a complex near-surface, you may need to perform dynamic rather than statics corrections for the near-surface.
- Irregular topography with significant elevation differences within a spread length prohibits the use of CMP datum for velocity analysis. As such, you need to perform velocity estimation from topography.
- Migration from a flat reference datum causes mispositioning of even flat reflectors. As such, you need to perform imaging from topography.

A velocity-depth model for the subsurface is defined by two sets of parameters - layer velocities and reflector geometries. The workflow described in this essay uses *image-based* velocity estimation and reflector geometry delineation. This is based on the observation that, aside from imaging in time and in depth, prestack time and depth migrations can also be used to estimate RMS and interval velocities, and verify the accuracy of the RMS and interval velocity fields based on flatness of events on image gathers.

Specifically, RMS velocities are picked from a velocity cube generated by prestack time migration of shot gathers from topography. This guarantees estimation of RMS velocities at reflector positions, not at reflection positions. Interval velocities are either derived from Dix conversion of the RMS velocities or they are picked from a velocity cube generated by prestack depth migration of shot gathers from topography. Again, this guarantees estimation of interval velocities at reflector positions. There is, however, an important difference between the image-based RMS and interval velocity estimation: the latter is performed layer-by-layer. Reflector geometries are delineated by picking depth horizons from image sections created by poststack or prestack depth migration.

An earth modelling project involves model building, model updating, model verification, and model calibration to well tops. A brief description of each phase in earth modelling is given below.

Model building requires combining inversion methods to estimate layer velocities and delineate reflector geometries. The most robust combination for 2D seismic data is Dix conversion of RMS velocities to determine layer velocities and poststack depth migration to pick depth horizons that represent the reflector geometries. The crucial point to keep in mind is that the RMS velocities must be estimated at reflector positions. It is incorrect to perform Dix conversion of stacking or DMO velocities, even after some smoothing, as they are estimated at reflection positions. The combination of Dix conversion with poststack depth migration may work for a complex subsurface structure, but not for a complex *overburden* structure. For example, use this combination to model the overburden above a salt diapiric structure or an overthrust imbricate structure. But when dealing with a target *beneath* such complex overburden structures, then you will need the *layer-by-layer* application of combination of half-space velocity analysis to determine the layer velocities and prestack depth migration to pick the depth horizon that represent the reflector geometry of the base of the layer under consideration.

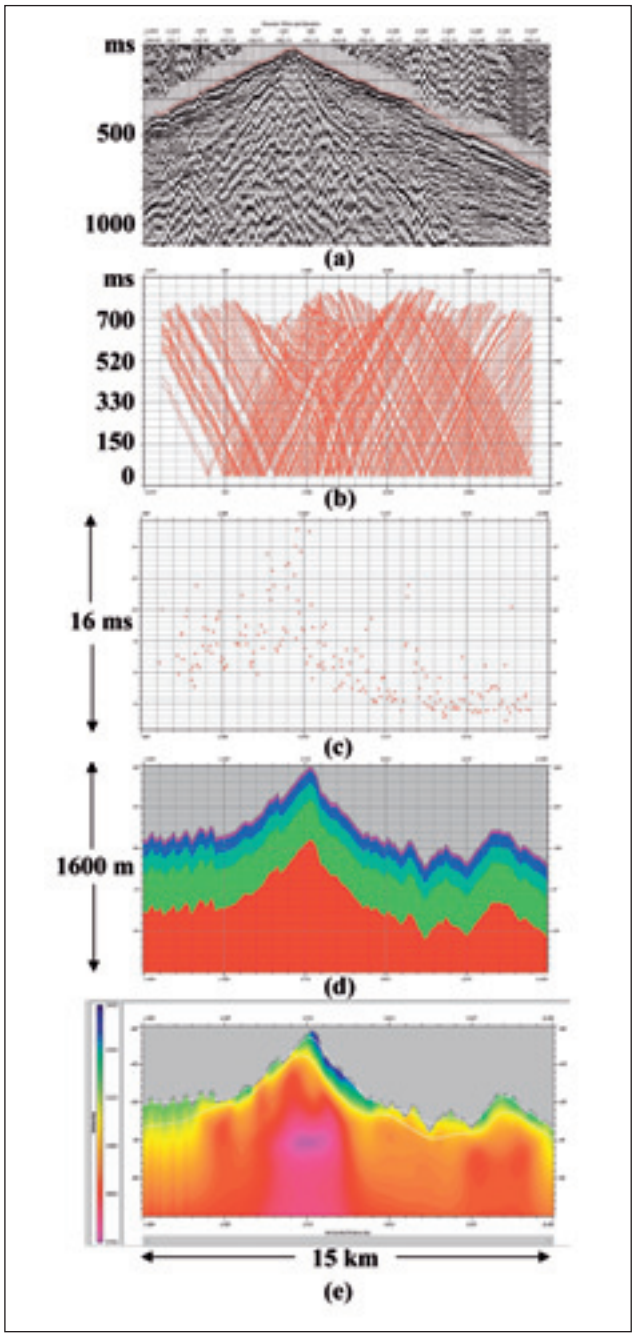

Figure 1 *(a) A shot record with first-break picks (offset range shown is approximately from –1.6 km to 2.7 km); (b) First-arrival times along a seismic line traverse picked from all shots; (c) average reciprocal errors for all shots as in (b); (d) initial model for the near-surface (elevation difference along the line traverse is nearly 700 m); and (e) final model for the near-surface estimated by nonlinear traveltime tomography using the first-arrival times in (b) and the initial model in (d). Note the high-velocity intrusion at the center (velocities vary between 1500-5500 m/s). The two white horizons represent the floating and intermediate datum.*

Model updating requires residual moveout analysis of image gathers derived from prestack depth migration and correcting for errors in velocities and/or reflector depths. The process essentially involves transformation of residual moveouts to changes in layer velocities and layer thicknesses, and it can be applied either locally or globally. In the former mode, model parameters are updated at each image-gather location, independently. In the latter mode, model parameters are updated by reflection tomography in which a residual moveout at one location affects the perturbation of the model parameters at another location.

Model verification requires flatness of events on image gathers from prestack depth migration and consistency of the modelled zero-offset traveltimes with the observed traveltimes on demigrated data associated with the reflectors which were included in the initial model. Consistency between modelled and observed traveltimes is necessary but not a sufficient condition to resolve the velocity-depth ambiguity in model building. This ambiguity arises for a fundamental reason: an error in reflector geometry is indistinguishable from an error in velocity. The velocity-depth ambiguity is infinite in case of a zero-offset wavefield represented approximately by CMP stacked data. You can have an infinite number of velocity-depth models which are all consistent with your stacked data, but none of them may closely represent the true geological model. To resolve the velocity-depth ambiguity; that is, to reduce the infinite number of solutions to a few, you need to record with as many offsets and as large offsets as possible, then perform earth modelling using prestack data and imaging by prestack, not poststack, depth migration. As a result, you will be able to better detect flatness of events on image gathers and thus verify the accuracy of your model and the fidelity of your image.

Model calibration is required to match the depth structure map you generate from the depth images along each of the lines in a multi-line 2D survey to 'the ground truth' - the well tops. The key issue here is dealing with the sparseness of the well data versus the relatively high-density surface seismic data. Matching two such incompatible sets of information is done by krigging.

Following this overview of earth modelling, we now describe the workflow for 2D land data processing, broken down into 13 steps.

Near-surface modelling

First break picking (step 1). Starting with the field records with geometry in trace headers, pick first-arrival times (Figure 1a), and edit traces for high noise level or for lack of signal, and for polarity reversals. When picking first-arrival times, you may wish to use manual, semi-automatic, or automatic picking strategies depending on the quality of the first breaks. Whatever the strategy, picking stage is when you also first become acquainted with the nature of the noise and signal in your data.

Building initial model for the near-surface (step 2). Combine all the picked first-arrival times (Figure 1b), and edit for bad picks. Check the reciprocal errors and make sure that they are sufficiently small. In general, the maximum reciprocal error should be less than 20 ms, and the average of the reciprocal errors for all shots should be less than 10 ms. In theory, reciprocity principal states that interchanging shot and receiver locations does not alter the first-arrival traveltime. However, in practice, errors in geometry, irregularities in geometry, charge depth, mispicks, and heterogeneities in the vicinity of the shot and receiver locations can cause differences between the reciprocal times. Large reciprocal errors are often caused by geometry and/or picking errors. Therefore, the reciprocal error display (Figure 1c) and the shot-receiver location diagram along the line traverse are used to quality control the geometry and traveltime picks. Next, bundle the traveltime trajectories to form a general trend that can be associated with laterally invariant but vertically varying velocities within the near surface. Pick a traveltime trajectory while honouring the change in gradient. Determine the near-surface layer velocities and thicknesses inferred by the picked traveltime trajectory. Then, build an initial model (Figure 1d) for the near-surface based on these layer velocities and thicknesses. After estimating the final velocity-depth model for the near-surface by way of nonlinear traveltime tomography

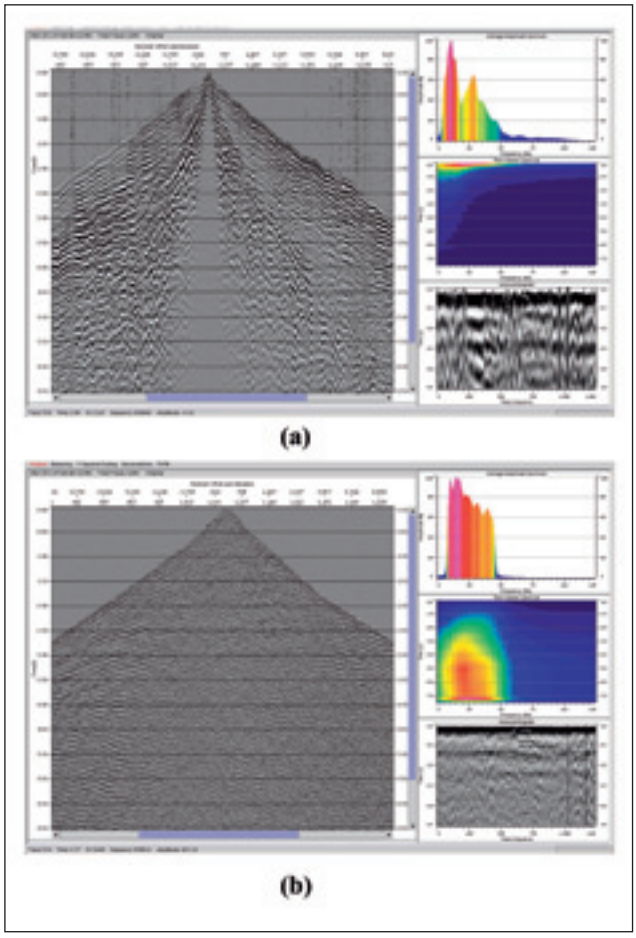

Figure 2 *(a) A shot gather with its average amplitude spectrum (top right), time-variant spectrum (center-right), and autocorrelogram (bottom-right); and (b) the same shot gather after t-squared scaling, deconvolution, time-variant spectral whitening, statics corrections, and f-x prediction filtering to remove the residual coherent linear noise associated with ground-roll energy.*

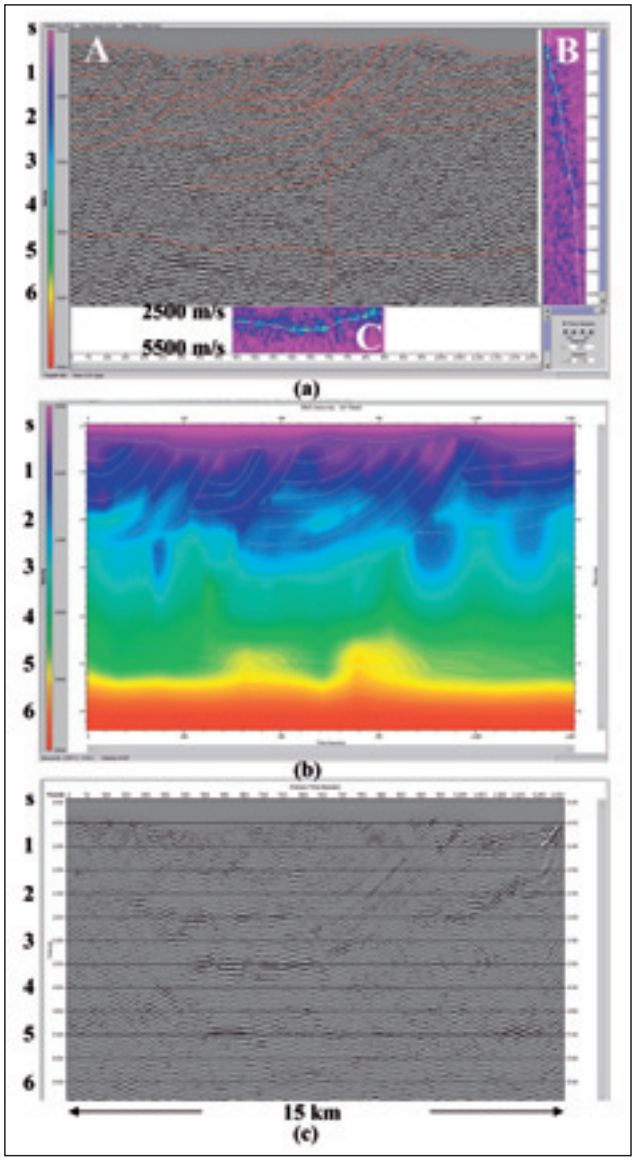

Figure 3 *(a) Three cross-sections of a velocity cube in time --- A: image panel for a specific velocity, B: semblance spectrum at a specific location along the line traverse, and C: time slice or horizon-consistent semblance spectrum; (b) the RMS velocity strands and the RMS velocity field derived from the velocity cube in (a); and (c) image from prestack time migration using the RMS velocity field in (b).*

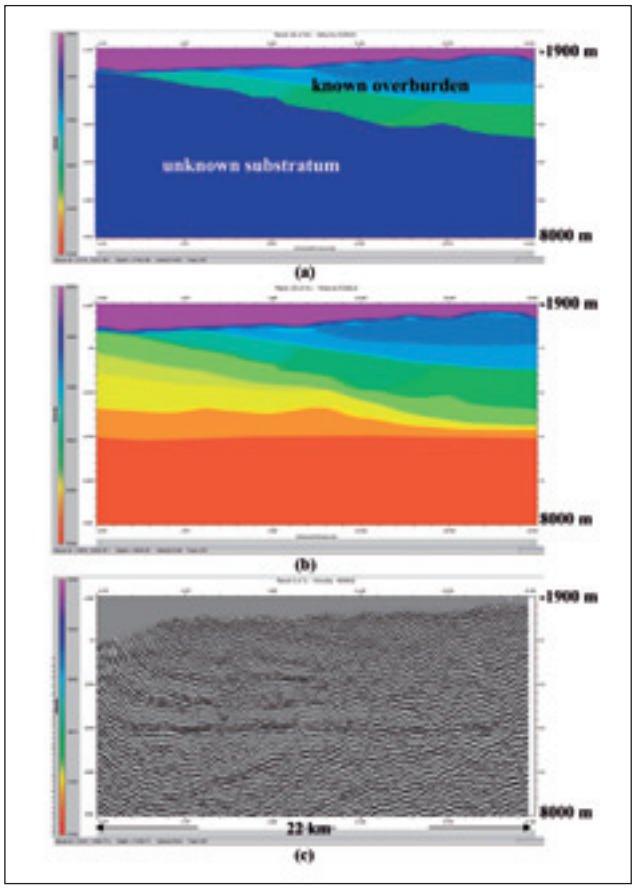

Figure 4 *(a) A velocity-depth model at an intermediate stage of model building based on layer-by-layer estimation of layer velocities and delineation of reflector geometries; (b) final velocity-depth model; and (c) image from prestack depth migration using the velocity-depth model in (b).*

in step 3, examine the discrepancy between the observed (picked) traveltimes and modeled traveltimes associated with the final velocity-depth model.

Estimation of the near-surface model by nonlinear traveltime tomography (step 3). Perform ray tracing to compute the traveltimes associated with the initial velocity-depth model using the shot and receiver locations. Then, perturb the initial model parameters until the difference between the modelled and the picked traveltimes is minimum in the least-squares sense using nonlinear traveltime tomography that accounts for changes in traveltime gradient (Zhang and Toksoz, 1998). Iterate until the discrepancy between the modelled and the picked traveltimes, measured as the RMS error in inversion, has been reduced to a sufficiently small value comparable to the reciprocal errors.

Picking floating datum and intermediate datum (step 4). View the near-surface model (Figure 1e) derived by the nonlinear traveltime tomography, and pick the floating datum that is a smoothed form of the topography and the intermediate datum that defines the interface between the near-surface with relatively low velocities and the subsurface. Also, compute the replacement velocity taken as the lateral average of the velocities along the intermediate datum. Examine the raypaths associated with the near-surface model and make sure that they do not hit the bottom of the model. This is an indispensable quality control to judge as to the acceptance of the near-surface model. Also, examine the discrepancy between the modelled traveltimes associated with the tomography solution for the near-surface and the picked traveltimes, and make sure that the match between the modelled and the picked traveltimes is satisfactory.

Calculating Statics (step 5). Using the near-surface model estimated in step 3, the floating datum and intermediate datum picked in step 4, and the replacement velocity determined in step 4, compute the shot and receiver statics. The computation is in two steps: first, shots and receivers are moved down from topography to the intermediate datum using the velocity field associated with the near-surface; second, they are moved up to the floating datum using the replacement velocity. The shot and receiver statics are to be applied in the next step. At this stage, you can also calculate refraction-based shot and receiver residual statics (Zhang and Yilmaz, 2005).

RMS velocity estimation and prestack time migration

Signal Processing (step 6). Perform signal processing of the edited shot records from step 1. After each process, examine the average amplitude spectrum, time-variant spectrum, and the autocorrelogram for assessment and quality control of the processing parameters (Figure 2). The signal processing for typical land data may include resampling, inside muting for surface waves and outside trace muting, *t*-squared scaling for spherical spreading compensation, predictive deconvolution to compress the source wavelet to a desired length and attenuate short-period multiples and reverberations, time-variant spectral whitening to account for signal non-stationarity and thus flatten the spectrum within the recoverable signal passband, bandpass filtering, AGC, and *f-x* dip filtering (Wang, 1991) of coherent linear noise such as surface waves. Using the data attributes - average amplitude spectrum, time-variant spectrum, and autocorrelogram - we can decide on an optimum signal processing sequence with appropriate parameters. At this stage, you also apply statics corrections calculated in step 5.

Creating the velocity cube for RMS velocity picking (step 7). Perform prestack time migration of shot gathers from the floating datum using a constant velocity and sum the individual images from all the shot gathers to obtain a composite image of the subsurface. Repeat this process for a range of constant velocities and thus obtain a set of multiple images of the subsurface. By placing these constant-

velocity image panels together, you create a velocity cube (Shurtleff, 1984; Yilmaz, 2001), which is then interpreted in the next step to derive an RMS velocity field associated with events in their migrated positions. This RMS velocity field is better suited for Dix conversion to derive an interval velocity field (step 11) compared to Dix conversion of stacking or DMO velocities, which are associated with events in their unmigrated positions.

Creating the RMS velocity field (step 8). Display the three cross-sections of the velocity cube for picking the RMS velocities (Figure 3a) - A: image panel for a specific velocity, B: semblance spectrum at a specific location along the line traverse, and C: time slice or horizon-consistent semblance spectrum (Yilmaz et al., 2005a, b; Nicanoff et al., 2006). Scan the image panels (A) and pick horizon strands associated with the best image with the highest amplitude. Then, pick the velocity strand associated with each horizon strand from the horizon-consistent semblance spectrum (B). Use the semblance spectrum (C) for quality control of the picked velocity strands. While the image panels provide structural consistency, the time slices or horizon-consistent semblance spectra provide the lateral consistency in picking the velocity strands. After picking all the time horizon and RMS velocity strands, create an RMS velocity field associated with events in their migrated positions (Figure 3b).

Prestack time migration (step 9). Migrate the shot gathers from step 6 from the floating datum, individually, using the RMS velocity field from step 8 and sort the shot images to common-receiver gathers (Reshef and Kosloff, 1986; Yilmaz, 2001). Each trace in a common-receiver gather represents the subsurface image beneath the receiver location contributed by a particular shot. If the RMS velocity field is defined correctly, then the traces in a common-receiver gather can be treated as the replicas of the same subsurface image. Thus, events on a common-receiver gather should be flat with no residual moveout. To obtain the image from prestack time migration, simply stack the traces in each common-receiver gather (Figure 3c).

Demigration (step 10). Unmigrate the resulting image from prestack time migration using the same RMS velocity field (step 8) as for prestack time migration. The demigrated section is a representation of a zero-offset wavefield; as such, it is the appropriate input to poststack depth migration (step 11) compared to the conventional stack, which is only an approximate representation of a zero-offset section.

Velocity-depth model estimation and prestack depth migration

Earth modelling in depth (step 11). You may choose two different strategies for earth modelling in depth: (a) Perform Dix conversion of the RMS velocities from step 8 to derive an interval velocity field. Next, perform poststack depth migration of the demigrated section from step 10 using the interval velocity field. Overlay the image from poststack depth migration and the interval velocity field to check for consistency of the earth image with the earth model. Then, interpret a set of depth horizons associated with layer boundaries with significant velocity contrast. Divide each layer into a set of thin layers by creating phantom horizons so as to preserve the fine-grained vertical and lateral velocity variations within each layer inferred by the interval velocity field. (b) Alternatively, perform earth modelling by constant-half-space velocity analysis, layer-by-layer starting with the near-surface model at the top. Consider an intermediate stage in the analysis whereby you have already estimated a portion of the earth model from the top (Figure 4a). Assign

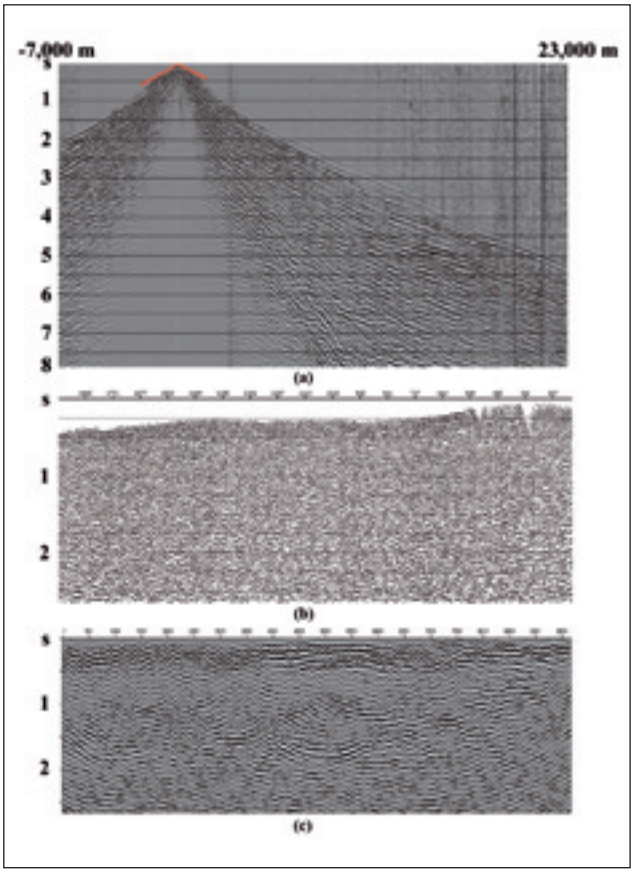

Figure 5 *(a) A large-offset shot gather acquired by a common receiver-spread recording geometry with 30-km maximum offset (note the wide-angle reflection at large offsets); (b) image from poststack time migration of data acquired by conventional CMP recording geometry and processed in midpoint-offset coordinates; and (c) image from prestack time migration of large-offset data acquired by common-receiver spread recording geometry (note the imbricate structures at the center associated with overthrust tectonics).*

a constant velocity or constant vertical gradient to the half-space that represents the underlying substratum with layers yet to be resolved. Perform prestack depth migration using the known overburden model and the underlying constant-velocity or constant-gradient half-space. Repeat prestack depth migration using the same overburden model but with different half-space velocities or gradients and collect the image panels in the form of a velocity cube in depth. Convert the image panels from depth to time and pick the event associated with the base of the layer under consideration. Then, extract the horizon-consistent semblance spectrum from the velocity cube and pick the interval velocity or gradient strand along the line traverse. Assign the estimated interval velocity field to the half-space and perform prestack depth migration to pick the horizon strand associated with the base of the layer under consideration, now in depth. Combine the interval velocity strand and the depth horizon strand to build a new velocity-depth model in which the estimated layer is now part of the known overburden model. Repeat this exercise for each of the layers under consideration to estimate the final model layer-by-layer, alternating between velocity estimation and reflector geometry delineation (Figure 4b).

Prestack depth migration (step 12). Perform depth migration of the shot gathers from step 6 from the floating datum, individually, and sort the shot images to common-receiver gathers in depth (Reshef and Koslof, 1986; Yilmaz, 2001). Each trace in a common-receiver gather represents the subsurface image beneath the receiver location contributed by a particular shot. If the interval velocity field is defined correctly, then the traces in a common-receiver gather can be treated as the replicas of the same subsurface image in depth. Thus, events on a common-receiver gather should be flat with no residual moveout. To obtain the image from prestack depth migration, simply stack the traces in each common-receiver gather.

Postmigration signal processing (step 13). Apply appropriate signal processing to the outputs from prestack time migration (step 9), demigration (step 10), poststack depth migration (step 11), and prestack depth migration (step 12). The signal processing may include predictive deconvolution to restore the flatness of the spectrum within the signal passband, time-variant spectral whitening to account for signal nonstationarity, bandpass filtering, *f-x* deconvolution (Canales, 1984) for attenuation of random noise uncorrelated from trace to trace, and AGC. Using the data attributes - average amplitude spectrum, time-variant spectrum, and autocorrelogram - we can decide on an optimum signal processing sequence with appropriate parameters. Additionally, you can perform residual statics corrections and/or residual inversion for model and image updating on the gathers from prestack time and depth migrations.

Aspects of land data acquisition

Implications of land data processing on data acquisition are briefly discussed below.

To circumvent spatial aliasing in prestack time and depth migrations, you need to record the data with sufficiently small receiver group interval. Since, both prestack time and depth migrations are performed by migrating individual shot gathers independent of each other, you do not need to be concerned with the shot spacing: it can be irregular or coarse because of difficult ground conditions.

To attain the desired resolution in velocity estimation and model verification, you need to record with as many offsets and as large offsets as possible. Moreover, you are not bound by the small-spread approximation in NMO correction, since the workflow described in this essay does not include NMO correction and stacking.

Rayleigh-type surface-wave energy often can overwhelm the weak subcritical reflection energy. Although you may be able to partially attenuate the ground-roll energy by receiver arrays in the field, they cannot be entirely eliminated. Hence, you need to apply multichannel filters such as *f-x* prediction filter (Wang, 1991) or correlation filter using seismic interferometry (Schuster et al., 2006), to attenuate the ground-roll energy during processing.

P-to-P reflection amplitudes are much larger beyond the critical angle of incidence compared to those within the subcritical region of propagation. Although supercritical reflections are much lower in frequency content because of intrinsic attenuation in rocks, they have sufficiently strong amplitudes that can survive the deleterious effect of ambient noise and the ground-roll energy. Moreover, if you record with super-large offsets beyond 12 km, then you avoid the ground-roll energy altogether (Figure 5a). Large-offset seismic surveys can be conducted using common-receiver spread recording geometry. This reduces the acquisition cost while providing high-fold coverage. The resulting image from a large-offset survey (Colombo et al., 2003; Yilmaz et al., 2005a; Yilmaz et al., 2005b) can be surprisingly superior to that from a survey with a conventional spread (Figures 5b,c).

Conclusions

The deliverables from the workflow described in this essay include: the near-surface model, the RMS velocity field estimated at the reflector positions, the image from prestack time migration, the demigrated section, the interval velocity field estimated at the reflector positions, the image from poststack depth migration, and the image from prestack depth migration. We model the near-surface by nonlinear traveltime tomography applied to first arrivals. We model the subsurface by image-based estimation of RMS and interval velocities and, again, image-based delineation of reflector geometries.

The workflow offers two strategies for earth modelling in depth: (1) A combination of Dix conversion of RMS

velocities to determine layer velocities and poststack depth migration to pick depth horizons that represent the reflector geometries. This strategy may work for a complex subsurface structure, but not for a complex *overburden* structure. (2) A *layer-by-layer* application of combination of half-space velocity analysis to determine the layer velocities and prestack depth migration to pick the depth horizon that represent the reflector geometry of the base of the layer under consideration. This combination is imperative when dealing with a target *beneath* complex overburden structures.

Acknowledgements

We thank TPAO, Repsol, ONGC, and CNPC for giving us the opportunity to implement the workflow described in this essay on their data and granting the permission to publish the results.

References

Canales, L. [1984] Random noise reduction. *54th SEG Annual International Meeting, Atlanta.* Expanded Abstracts.

Colombo, D., Wilkes, M., Villani, L., and Mantovani, M. [2003] *73rd SEG Annual International Meeting.* Expanded Abstracts

Nicanoff, L., Perez, Y., Yilmaz, O., Dai, N., and Zhang, J. [2006] A case study for imaging complex structures in the Andean Thrust Belt of Bolivia, *76th SEG Annual International Meeting, New Orleans*. Expanded Abstracts.

Reshef, M. and Kosloff, D. [1986] Migration of common-shot gathers, *Geophysics*, 51.

Schuster, G. T., Shuqian, D., and Reiqing, H. [2006] Intrerferometric prediction and least-squares subtraction of surface waves. *76th SEG Annual International Meeting*, *New Orleans*. Expanded Abstracts.

Shurtleff, R. [1984] *An F-K procedure for prestack migration and velocity analysis*. 46th EAEG Annual Meeting.

Wang, W. [1991] *F-X filters with dip rejection, 61st SEG Annual International Meeting, Houston.* Expanded Abstracts.

Yilmaz, O. [2001] *Seismic Data Analysis*. SEG, Tulsa.

Yilmaz, O., Zhang, J., Pince, A., Aytunur, A., Elibuyuk, A., Uygun, S., Onaran, T., and Oner, A. F. [2005a] *A large-offset 2-D seismic survey for imaging complex structures in thrust belts. 75th SEG Annual International Meeting, Houston.* Expanded Abstracts.

Yilmaz, O., Zhang, J., and Shixin, Y. [2005b] *Acquisition and processing of large-offset seismic data: a case study from Northwest China. 75th SEG Annual International Meeting, Houston.* Expanded Abstracts.

Zhang, J. and Toksoz, M. N. [1998] *Nonlinear refraction traveltime tomography*. Geophysics, 63.

Zhang, J. and Yilmaz, O. [2005] *Near-surface corrections for complex structure imaging. 76th SEG Annual International Meeting, Houston.* Expanded Abstracts.